A globally divergence-free discontinuous galerkin method for induction and related equations

Praveen Chandrashekar
praveen@math.tifrbng.res.in

Center for Applicable Mathematics
Tata Institute of Fundamental Research
Bangalore-560065, India
http://cpraveen.github.io

Int. Conf. on Current Trends in Theoretical and Computational Differential Equations with Applications, SAU, New Delhi
1–5 December 2017

Supported by Airbus Foundation Chair at TIFR-CAM, Bangalore
http://math.tifrbng.res.in/airbus-chair

Joint work with
Dinshaw Balsara
Univ. of Notre Dame

Maxwell Equations

Linear hyperbolic system

$$\frac{\partial \boldsymbol{B}}{\partial t} + \nabla \times \boldsymbol{E} = 0, \qquad \frac{\partial \boldsymbol{D}}{\partial t} - \nabla \times \boldsymbol{H} = -\boldsymbol{J}$$

$\boldsymbol{B}$ = magnetic flux density
$\boldsymbol{E}$ = electric field
$\boldsymbol{D}$ = electric flux density
$\boldsymbol{H}$ = magnetic field
$\boldsymbol{J}$ = electric current density

$$\boldsymbol{B} = \mu \boldsymbol{H}, \qquad \boldsymbol{D} = \varepsilon \boldsymbol{E}, \qquad \boldsymbol{J} = \sigma \boldsymbol{E} \qquad \mu, \varepsilon \in \mathbb{R}^{3\times 3} \text{ symmetric}$$

ε = permittivity tensor
μ = magnetic permeability tensor
σ = conductivity

$$\nabla \cdot \boldsymbol{B} = 0, \quad \nabla \cdot \boldsymbol{D} = \rho \quad \text{(electric charge density)}, \quad \frac{\partial \rho}{\partial t} + \nabla \cdot \boldsymbol{J} = 0$$

Ideal MHD equations

Nonlinear hyperbolic system

Compressible Euler equations with Lorentz force

$$
\begin{aligned}
\frac{\partial \rho}{\partial t} + \nabla \cdot (\rho \boldsymbol{v}) &= 0 \\
\frac{\partial \rho \boldsymbol{v}}{\partial t} + \nabla \cdot (pI + \rho \boldsymbol{v} \otimes \boldsymbol{v} - \boldsymbol{B} \otimes \boldsymbol{B}) &= 0 \\
\frac{\partial E}{\partial t} + \nabla \cdot ((E + p)\boldsymbol{v} + (\boldsymbol{v} \cdot \boldsymbol{B})\boldsymbol{B}) &= 0 \\
\frac{\partial \boldsymbol{B}}{\partial t} - \nabla \times (\boldsymbol{v} \times \boldsymbol{B}) &= 0
\end{aligned}
$$

Magnetic monopoles do not exist: $\implies \quad \nabla \cdot \boldsymbol{B} = 0$

Model problem

$$\frac{\partial \boldsymbol{B}}{\partial t} + \nabla \times \boldsymbol{E} = -\boldsymbol{M}$$

Divergence evolves according to

$$\frac{\partial}{\partial t}(\mathrm{div}\boldsymbol{B}) + \nabla \cdot \boldsymbol{M} = 0 \tag{1}$$

In 2-D

$$\frac{\partial B_x}{\partial t} + \frac{\partial E_z}{\partial y} = -M_x, \qquad \frac{\partial B_y}{\partial t} - \frac{\partial E_z}{\partial x} = -M_y$$

Model problem

In MHD, $\boldsymbol{B}$ represents the magnetic field and $\boldsymbol{M} = 0$

$$\frac{\partial \boldsymbol{B}}{\partial t} + \nabla \times \boldsymbol{E} = 0, \qquad \boldsymbol{E} = -\boldsymbol{v} \times \boldsymbol{B}$$

Magnetic monopoles do not exist: $\implies$ $\nabla \cdot \boldsymbol{B} = 0$
If

$$\nabla \cdot \boldsymbol{B} = 0 \qquad \text{at} \quad t = 0$$

then

$$\frac{\partial}{\partial t}(\nabla \cdot \boldsymbol{B}) + \nabla \cdot \nabla \times \boldsymbol{E} = 0 \quad \implies \quad \nabla \cdot \boldsymbol{B} = 0 \quad \text{for} \quad t > 0$$

In 2-D, the induction equation can be written as

$$\frac{\partial B_x}{\partial t} + \frac{\partial E}{\partial y} = 0, \qquad \frac{\partial B_y}{\partial t} - \frac{\partial E}{\partial x} = 0, \qquad E = v_y B_x - v_x B_y$$

Some existing methods for MHD

Exactly divergence-free methods

- Constrained transport ([1] Evans & Hawley (1989))
  - $\nabla \cdot \boldsymbol{B} = 0$ implies $\boldsymbol{B} = \nabla \times \boldsymbol{A}$
  - Evolve $\boldsymbol{A}$ forward in time
  - Compute $\boldsymbol{B}$ from $\boldsymbol{A}$
- Divergence-free reconstruction ([2] Balsara (2001))
- Globally divergence-free scheme ([3] Li et al. (2011))

Approximate methods

- Using Godunov's symmetrized version of MHD [4] (Powell [5], CK [6])
- Divergence cleaning methods (Dedner et al. [7])

Approximation of magnetic field

When dealing with problems where the vector field $\boldsymbol{B}$ must be divergence-free, it is natural to look for solutions in $H(\mathrm{div}, \Omega)$ which is defined as

$$H(\mathrm{div}, \Omega) = \{\boldsymbol{B} \in \boldsymbol{L}^2(\Omega) : \mathrm{div}(\boldsymbol{B}) \in L^2(\Omega)\}$$

To approximate functions in $H(\mathrm{div}, \Omega)$ on a mesh $\mathcal{T}_h$, we need the following compatibility condition.

Theorem (See [8], Proposition 3.2.2)

Let $\boldsymbol{B}^h : \Omega \to \mathbb{R}^d$ be such that

1. $\boldsymbol{B}^h|_K \in \boldsymbol{H}^1(K)$ *for all* $K \in \mathcal{T}_h$
2. *for each common face* $F = K_1 \cap K_2$, $K_1, K_2 \in \mathcal{T}_h$, *the trace of normal component* $\boldsymbol{n} \cdot \boldsymbol{B}^h|_{K_1}$ *and* $\boldsymbol{n} \cdot \boldsymbol{B}^h|_{K_2}$ *is the same.*

Then $\boldsymbol{B}^h \in H(div, \Omega)$. Conversely, if $\boldsymbol{B}^h \in H(div, \Omega)$ and (1) holds, then (2) is also satisfied.

Approximation of magnetic field

$P_k(x)$, $P_k(y)$: 1-D polynomials of degree at most k wrt the variables x, y respectively.

$Q_{r,s}(x,y)$: tensor product polynomials of degree r in the variable x and degree s in the variable y, i.e.,

$$Q_{r,s}(x,y) = \mathrm{span}\{x^i y^j,\ 0 \le i \le r,\ 0 \le j \le s\}$$

For $k \ge 0$, the Raviart-Thomas space of vector functions is defined as

$$\mathbf{RT}_k = Q_{k+1,k} \times Q_{k,k+1}, \qquad \dim(\mathbf{RT}_k) = 2(k+1)(k+2)$$

Two consequences:

- For any $\boldsymbol{B}^h \in \mathbf{RT}_k$, we have

$$\mathrm{div}(\boldsymbol{B}^h) \in Q_{k,k}(x,y) =: Q_k(x,y)$$

Approximation of magnetic field

- The restriction of $\boldsymbol{B}^h = (B_x^h, B_y^h)$ to a face is a polynomial of degree k, i.e.,

$$B_x^h(\pm\Delta x/2, y) \in P_k(y), \qquad B_y^h(x, \pm\Delta y/2) \in P_k(x)$$

For doing the numerical computations, it is useful to map each cell to a reference cell.

$$\{\xi_i, 0 \le i \le k+1\} = \text{Gauss-Lobatto-Legendre (GLL) nodes}$$

$$\{\hat{\xi}_i, 0 \le i \le k\} = \text{Gauss-Legendre (GL) nodes}$$

Let ϕ_i and $\hat{\phi}_i$ be the corresponding 1-D Lagrange polynomials. Then the magnetic field is given by

$$B_x^h(\xi,\eta) = \sum_{i=0}^{k+1}\sum_{j=0}^{k}(B_x)_{ij}\phi_i(\xi)\hat{\phi}_j(\eta), \quad B_y^h(\xi,\eta) = \sum_{i=0}^{k}\sum_{j=0}^{k+1}(B_y)_{ij}\hat{\phi}_i(\xi)\phi_j(\eta)$$

Approximation of magnetic field

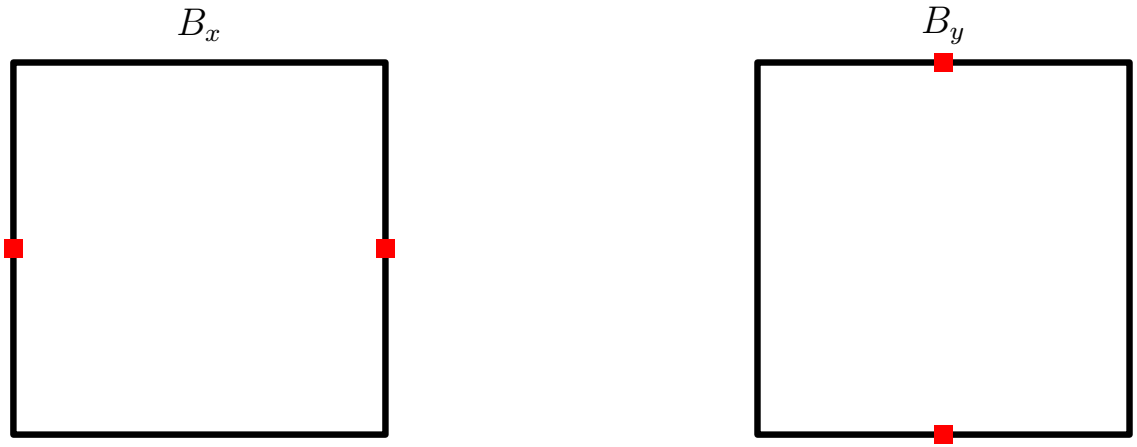

Location of dofs of Raviart-Thomas polynomial for $k = 0$

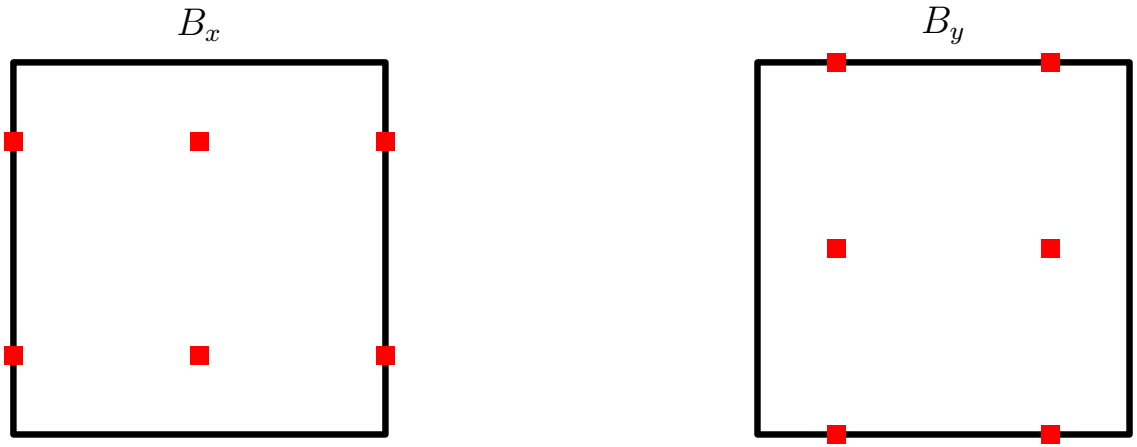

Location of dofs of Raviart-Thomas polynomial for $k = 1$

Approximation of magnetic field

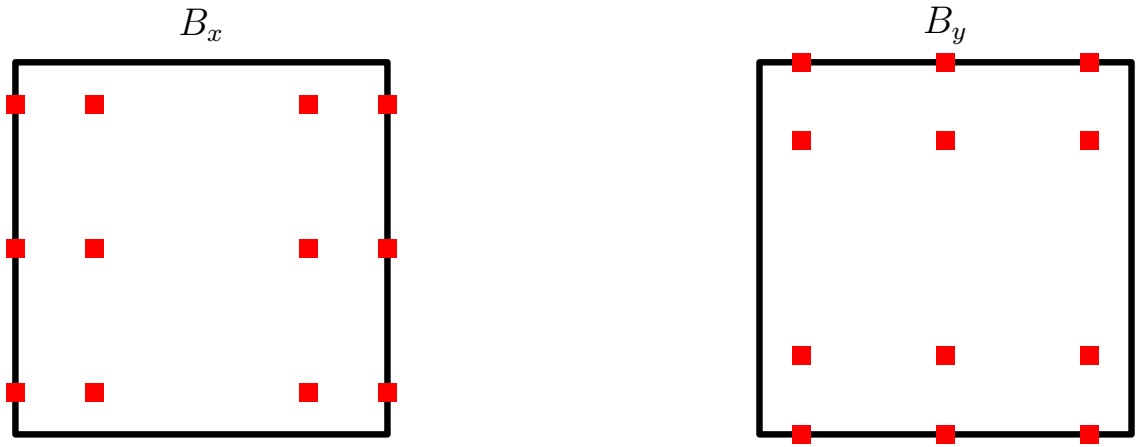

Location of dofs of Raviart-Thomas polynomial for $k = 2$

Our choice of nodes ensures that the normal component of the magnetic field is continuous on the cell faces.

We have the error estimates on Cartesian meshes [9], [10]

$$\|\boldsymbol{B} - \boldsymbol{B}^h\|_{\boldsymbol{L}^2(\Omega)} \leq Ch^{k+1}|\boldsymbol{B}|_{\boldsymbol{H}^{k+1}(\Omega)}$$

$$\|\mathrm{div}(\boldsymbol{B}) - \mathrm{div}(\boldsymbol{B}^h)\|_{\boldsymbol{L}^2(\Omega)} \leq Ch^{k+1}|\mathrm{div}(\boldsymbol{B})|_{\boldsymbol{H}^{k+1}(\Omega)}$$

Construction of $\boldsymbol{B}_h$ from moments

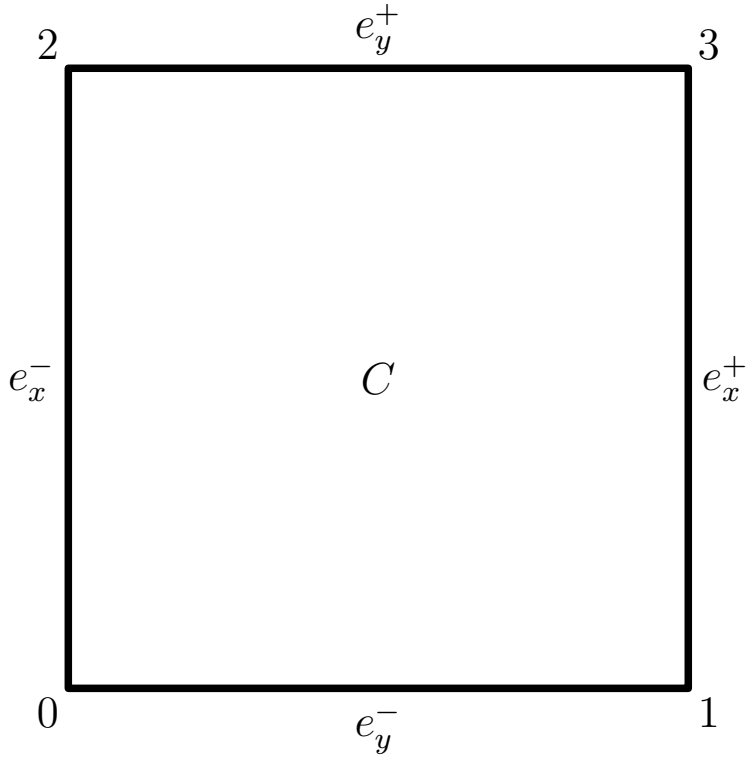

The edge moments are given by

$$\int_{e_x^{\mp}} B_x^h \phi \mathrm{d}y \qquad \forall \phi \in P_k(y)$$

and

$$\int_{e_y^{\mp}} B_y^h \phi \mathrm{d}x \qquad \forall \phi \in P_k(x)$$

The cell moments are given by

$$\int_C B_x^h \psi \mathrm{d}x \mathrm{d}y \qquad \forall \psi \in \partial_x Q_k(x,y) := Q_{k-1,k}(x,y)$$

Construction of $\boldsymbol{B}_h$ from moments

and

$$\int_C B_y^h \psi \mathrm{d}x\mathrm{d}y \qquad \forall \psi \in \partial_y Q_k(x,y) := Q_{k,k-1}(x,y)$$

Note that

$$\dim P_k(x) = \dim P_k(y) = k+1$$

and

$$\dim \partial_x Q_k(x,y) = \dim \partial_y Q_k(x,y) = k(k+1)$$

so that we have in total

$$4(k+1) + 2k(k+1) = 2(k+1)(k+2) = \dim \mathbf{RT}_k$$

The moments on the edges $e_x^{\mp}$ uniquely determine the restriction of B_x^h on those edges, and similarly the moments on $e_y^{\mp}$ uniquely determine the restriction of B_y^h on the corresponding edges. This ensures continuity of the normal component of $\boldsymbol{B}^h$ on all the edges.

Theorem

If all the moments are zero for any cell C, then $\boldsymbol{B}^h \equiv 0$ inside that cell.

Proof: The edge moments being zero implies that

$$B_x^h \equiv 0 \quad \text{on} \quad e_x^{\mp} \qquad \text{and} \qquad B_y^h \equiv 0 \quad \text{on} \quad e_y^{\mp}$$

Now take $\psi = \partial_x \phi$ for some $\phi \in Q_k$ in the cell moment equation of B_x^h and perform an integration by parts

$$-\int_C \frac{\partial B_x^h}{\partial x} \phi \mathrm{d}x\mathrm{d}y - \int_{e_x^-} B_x^h \phi \mathrm{d}y + \int_{e_x^+} B_x^h \phi \mathrm{d}y = 0$$

and hence

$$\int_C \frac{\partial B_x^h}{\partial x} \phi \mathrm{d}x\mathrm{d}y = 0 \qquad \forall \phi \in Q_k$$

Since $\frac{\partial B_x^h}{\partial x} \in Q_k$, this implies that $\frac{\partial B_x^h}{\partial x} \equiv 0$ and hence $B_x^h \equiv 0$. Similarly, we conclude that $B_y^h \equiv 0$. □

Theorem

Let $\boldsymbol{B}^h \in \mathbf{RT}_k$ *satisfy the moments*

$$\int_{e_x^{\mp}} B_x^h \phi \, dy = \int_{e_x^{\mp}} B_x \phi \, dy \qquad \forall \phi \in P_k(y) \tag{2}$$

$$\int_{e_y^{\mp}} B_y^h \phi \, dx = \int_{e_y^{\mp}} B_y \phi \, dx \qquad \forall \phi \in P_k(x) \tag{3}$$

$$\int_C B_x^h \psi \, dx dy = \int_C B_x \psi \, dx dy \qquad \forall \psi \in \partial_x Q_k(x,y) \tag{4}$$

$$\int_C B_y^h \psi \, dx dy = \int_C B_y \psi \, dx dy \qquad \forall \psi \in \partial_y Q_k(x,y) \tag{5}$$

for a given vector field $\boldsymbol{B} \in H(div, \Omega)$. *If* $div(\boldsymbol{B}) \equiv 0$ *then* $div(\boldsymbol{B}^h) \equiv 0$.

Proof: We choose $\psi = \partial_x \phi$ and $\psi = \partial_y \phi$ for some $\phi \in Q_k(x, y)$ respectively in the two cell moment equations (4), (5). Adding these two equations together, we get

$$\int_C (B_x^h \partial_x \phi + B_y^h \partial_x \phi) \mathrm{d}x\mathrm{d}y = \int_C (B_x \partial_x \phi + B_y \partial_y \phi) \mathrm{d}x\mathrm{d}y$$

Performing integration by parts on both sides

$$-\int_C \mathrm{div}(\boldsymbol{B}^h)\phi \mathrm{d}x\mathrm{d}y + \int_{\partial C} \phi \boldsymbol{B}^h \cdot \boldsymbol{n} \mathrm{d}s = -\int_C \mathrm{div}(\boldsymbol{B})\phi \mathrm{d}x\mathrm{d}y + \int_{\partial C} \phi \boldsymbol{B} \cdot \boldsymbol{n} \mathrm{d}s$$

Note that ϕ restricted to ∂C is a one dimensional polynomial of degree k and the edge moments of $\boldsymbol{B}^h$ and $\boldsymbol{B}$ agree with one another by equations (2), (3). Hence we get

$$\int_C \mathrm{div}(\boldsymbol{B}^h)\phi \mathrm{d}x\mathrm{d}y = \int_C \mathrm{div}(\boldsymbol{B})\phi \mathrm{d}x\mathrm{d}y \qquad \forall \phi \in Q_k(x, y)$$

If $\mathrm{div}(\boldsymbol{B}) \equiv 0$ then

$$\int_C \mathrm{div}(\boldsymbol{B}^h)\phi \mathrm{d}x\mathrm{d}y = 0 \qquad \forall \phi \in Q_k(x,y)$$

Since $\mathrm{div}(\boldsymbol{B}^h) \in Q_k(x,y)$ this implies that $\mathrm{div}(\boldsymbol{B}^h) \equiv 0$ everywhere inside the cell C. □

Remark: The proof makes use of integration by parts for which the quadrature must be exact. The integrals involving $\boldsymbol{B}^h$ can be evaluated exactly using Gauss quadrature of sufficient accuracy. This is not the case for the integrals involving $\boldsymbol{B}$ since it can be an arbitrary nonlinear function. When $\mathrm{div}(\boldsymbol{B}) = 0$, we have $\boldsymbol{B} = (\partial_y \Phi, -\partial_x \Phi)$ for some smooth function Φ. We can approximate Φ by $\Phi_h \in Q_{k+1}$ and compute the projections using $(\partial_y \Phi_h, -\partial_x \Phi_h)$ in which case the integrations can be performed exactly.

Example: $\mathbf{RT}_0$

$$B_x^h(x,y) = a_0 + a_1 x, \qquad B_y^h(x,y) = b_0 + b_1 y$$

In this case we have only the edge moments. The polynomial test function spaces needed to specify the edge moments are

$$P_0(x) = \text{span}\{1\}, \qquad P_0(y) = \text{span}\{1\}$$

and the four moments corresponding to the four faces are

$$\int_{-\frac{1}{2}}^{\frac{1}{2}} B_x^h(-1/2, y)\mathrm{d}y = \alpha_1 \qquad \int_{-\frac{1}{2}}^{\frac{1}{2}} B_x^h(1/2, y)\mathrm{d}y = \alpha_2$$

$$\int_{-\frac{1}{2}}^{\frac{1}{2}} B_y^h(x, -1/2)\mathrm{d}x = \beta_1 \qquad \int_{-\frac{1}{2}}^{\frac{1}{2}} B_y^h(x, 1/2)\mathrm{d}x = \beta_2$$

The solution is given by

$$a_0 = \tfrac{1}{2}(\alpha_1 + \alpha_2), \qquad a_1 = \alpha_2 - \alpha_1$$

$$b_0 = \tfrac{1}{2}(\beta_1 + \beta_2), \qquad b_1 = \beta_2 - \beta_1$$

Example: $\mathbf{RT}_1$

$$
\begin{aligned}
B_x^h(x,y) &= a_0 + a_1 x + a_2 y + a_3 xy + a_4(x^2 - \tfrac{1}{12}) + a_5(x^2 - \tfrac{1}{12})y \\
B_y^h(x,y) &= b_0 + b_1 x + b_2 y + b_3 xy + b_4(y^2 - \tfrac{1}{12}) + b_5 x(y^2 - \tfrac{1}{12})
\end{aligned}
$$

The polynomial test function spaces needed to specify the moments (2)-(5) are

$$P_1(x) = \mathrm{span}\{1, x\}, \qquad P_1(y) = \mathrm{span}\{1, y\}$$

$$\partial_x Q_1(x,y) = \mathrm{span}\{1, y\}, \qquad \partial_y Q_1(x,y) = \mathrm{span}\{1, x\}$$

Example: $\mathbf{RT}_2$

The polynomial test function spaces needed to specify the edge moments are

$$P_2(x) = \text{span}\{1, x, x^2 - \tfrac{1}{12}\}, \qquad P_2(y) = \text{span}\{1, y, y^2 - \tfrac{1}{12}\}$$

while those needed for the cell moments are given by

$$\partial_x Q_2(x, y) = \text{span}\{1, x, y, xy, y^2 - \tfrac{1}{12}, x(y^2 - \tfrac{1}{12})\}$$

$$\partial_y Q_2(x, y) = \text{span}\{1, x, y, xy, x^2 - \tfrac{1}{12}, (x^2 - \tfrac{1}{12})y\}$$

DG scheme for the induction equation

Constructing $\boldsymbol{B}^h$ from the edge and cell moments allowed us to get divergence-free approximation.

We will construct a scheme to evolve the same moments in time.

Edge moments are evolved by

$$\int_{e_x^{\mp}} \frac{\partial B_x^h}{\partial t}\phi \mathrm{d}y - \int_{e_x^{\mp}} \hat{E}\frac{\partial \phi}{\partial y}\mathrm{d}y + [\tilde{E}\phi]_{e_x^{\mp}} = -\int_{e_x^{\mp}} \hat{M}_x\phi \mathrm{d}y, \quad \forall \phi \in P_k(y)$$

$$\int_{e_y^{\mp}} \frac{\partial B_y^h}{\partial t}\phi \mathrm{d}x + \int_{e_y^{\mp}} \hat{E}\frac{\partial \phi}{\partial x}\mathrm{d}x - [\tilde{E}\phi]_{e_y^{\mp}} = -\int_{e_y^{\mp}} \hat{M}_y\phi \mathrm{d}y, \quad \forall \phi \in P_k(x)$$

where

$\hat{E} =$ numerical flux from a 1-D Riemann solver required on the faces

$\tilde{E} =$ numerical flux from a multi-D Riemann solver needed at vertices

DG scheme for the induction equation

$$[\tilde{E}\phi]_{e_x^-} = (\tilde{E}\phi)_2 - (\tilde{E}\phi)_0, \qquad [\tilde{E}\phi]_{e_x^+} = (\tilde{E}\phi)_3 - (\tilde{E}\phi)_1$$

$$[\tilde{E}\phi]_{e_y^-} = (\tilde{E}\phi)_1 - (\tilde{E}\phi)_0, \qquad [\tilde{E}\phi]_{e_y^+} = (\tilde{E}\phi)_3 - (\tilde{E}\phi)_2$$

The cells moments are evolved by the following standard DG scheme

$$\int_C \frac{\partial B_x^h}{\partial t}\psi \mathrm{d}x\mathrm{d}y - \int_C E\frac{\partial \psi}{\partial y}\mathrm{d}x\mathrm{d}y + \int_{\partial C} \hat{E}\psi n_y \mathrm{d}s = -\int_C M_x \psi \mathrm{d}x\mathrm{d}y, \quad \forall \psi \in \partial_x Q_k(x,y)$$

$$\int_C \frac{\partial B_y^h}{\partial t}\psi \mathrm{d}x\mathrm{d}y + \int_C E\frac{\partial \psi}{\partial x}\mathrm{d}x\mathrm{d}y - \int_{\partial C} \hat{E}\psi n_x \mathrm{d}s = -\int_C M_y \psi \mathrm{d}x\mathrm{d}y, \quad \forall \psi \in \partial_y Q_k(x,y)$$

Note that the same 1-D numerical flux $\hat{E}$ is used in both the edge and cell moment equations whereas the vertex numerical flux $\tilde{E}$ is needed only in the edge moment equations.

Theorem

Assuming that $\boldsymbol{M} = 0$, the DG scheme (22)-(22) preserves the divergence of the magnetic field.

Proof: For any $\phi \in Q_k(x, y)$ take $\psi = \partial_x \phi$ and $\psi = \partial_y \phi$ in the two cell moment equations respectively and add them together to obtain

$$\int_C \left[\frac{\partial B_x^h}{\partial t} \partial_x \phi + \frac{\partial B_y^h}{\partial t} \partial_y \phi \right] \mathrm{d}x\mathrm{d}y - \int_{\partial C} \hat{E}(n_x \partial_y \phi - n_y \partial_x \phi) \mathrm{d}s = 0$$

Note that two of the cell integrals cancel since $\partial_x \partial_y \phi = \partial_y \partial_x \phi$.
Performing an integration by parts in the first term, we obtain

$$-\int_C \phi \frac{\partial}{\partial t} \mathrm{div}(\boldsymbol{B}^h) \mathrm{d}x\mathrm{d}y + \int_{\partial C} \phi \frac{\partial}{\partial t} (\boldsymbol{B}^h \cdot \boldsymbol{n}) \mathrm{d}s - \int_{\partial C} \hat{E}(n_x \partial_y \phi - n_y \partial_x \phi) \mathrm{d}s = 0$$

Now, let us concentrate on the last two terms which can be re-arranged as follows

$$
\begin{aligned}
= & \int_{e_x^+} \phi \frac{\partial B_x^h}{\partial t} \mathrm{d}y - \int_{e_x^-} \phi \frac{\partial B_x^h}{\partial t} \mathrm{d}y + \int_{e_y^+} \phi \frac{\partial B_y^h}{\partial t} \mathrm{d}x - \int_{e_y^-} \phi \frac{\partial B_y^h}{\partial t} \mathrm{d}x \\
& - \int_{e_x^+} \hat{E} \partial_y \phi \mathrm{d}y + \int_{e_x^-} \hat{E} \partial_y \phi \mathrm{d}y + \int_{e_y^+} \hat{E} \partial_x \phi \mathrm{d}x - \int_{e_y^-} \hat{E} \partial_x \phi \mathrm{d}x \\
= & -[\tilde{E}\phi]_{e_x^+} + [\tilde{E}\phi]_{e_x^-} + [\tilde{E}\phi]_{e_y^+} - [\tilde{E}\phi]_{e_y^-} \\
= & -(\tilde{E}\phi)_3 + (\tilde{E}\phi)_1 + (\tilde{E}\phi)_2 - (\tilde{E}\phi)_0 + (\tilde{E}\phi)_3 - (\tilde{E}\phi)_2 - (\tilde{E}\phi)_1 + (\tilde{E}\phi)_0 \\
= & \ 0
\end{aligned}
$$

where we used the edge moment equations since the restriction of ϕ on each edge is a one dimensional polynomial of degree k. Hence we have

$$
\int_C \phi \frac{\partial}{\partial t} \mathrm{div}(\boldsymbol{B}^h) \mathrm{d}x \mathrm{d}y = 0 \qquad \forall \phi \in Q_k(x, y)
$$

Since $\mathrm{div}(\boldsymbol{B}^h) \in Q_k(x, y)$ we conclude that the divergence is preserved by the numerical scheme. □

Remark: The above proof required integration by parts in the terms involving the time derivative. These integrals can be computed exactly using Gauss quadrature of sufficient order. The other cell integral in the DG scheme can be computed using any quadrature rule of sufficient order and need not be exact. All the edge integrals which involve the numerical flux $\hat{E}$ appearing in the edge moment and cell moment evolution equations must be computed with the same rule and it is not necessary to be exact for the above proof to hold. However, from an accuracy point of view, these quadratures must be of a sufficiently high order to obtain optimal error estimates.

Remark: The preservation of divergence does not rely on the specific form of the fluxes $\tilde{E}$, $\hat{E}$ but only on the fact that we have a unique flux $\tilde{E}$ at all the vertices, and that we use the same 1-D numerical flux $\hat{E}$ in both the edge and cell moment equations.

Theorem ($\boldsymbol{M} \neq 0$)

The divergence evolves consistently with equation (1) in the sense that

$$\int_C \phi \frac{\partial}{\partial t} div(\boldsymbol{B}^h) dx dy - \int_C \boldsymbol{M} \cdot \nabla \phi dx dy + \int_{\partial C} \phi \hat{\boldsymbol{M}} \cdot \boldsymbol{n} ds = 0, \qquad \forall \phi \in Q_k$$

Since $div(\boldsymbol{B}^h) \in Q_k$*, we can expect* $div(\boldsymbol{B}^h)$ *to be accurate to* $O(h^{k+1})$*.*

Numerical fluxes

Using the zero divergence condition, rewrite the induction equation

$$\frac{\partial B_x}{\partial t}+\boldsymbol{v}\cdot\nabla B_x+B_x\frac{\partial v_y}{\partial y}-B_y\frac{\partial v_x}{\partial y}=0, \quad \frac{\partial B_y}{\partial t}+\boldsymbol{v}\cdot\nabla B_y+B_y\frac{\partial v_x}{\partial x}-B_x\frac{\partial v_y}{\partial x}=0$$

The characteristics are the integral curves of $\boldsymbol{v}$. The 1-D numerical flux is given by

$$\hat{E}=\begin{cases} E_L & \text{if } \boldsymbol{v}\cdot\boldsymbol{n}>0 \\ E_R & \text{otherwise} \end{cases}$$

For example, acorss the face $e_x^{\mp}$, the flux is given by

$$\hat{E}=\begin{cases} v_yB_x-v_xB_y^L & \text{if } v_x>0 \\ v_yB_x-v_xB_y^R & \text{otherwise} \end{cases}$$

Numerical fluxes

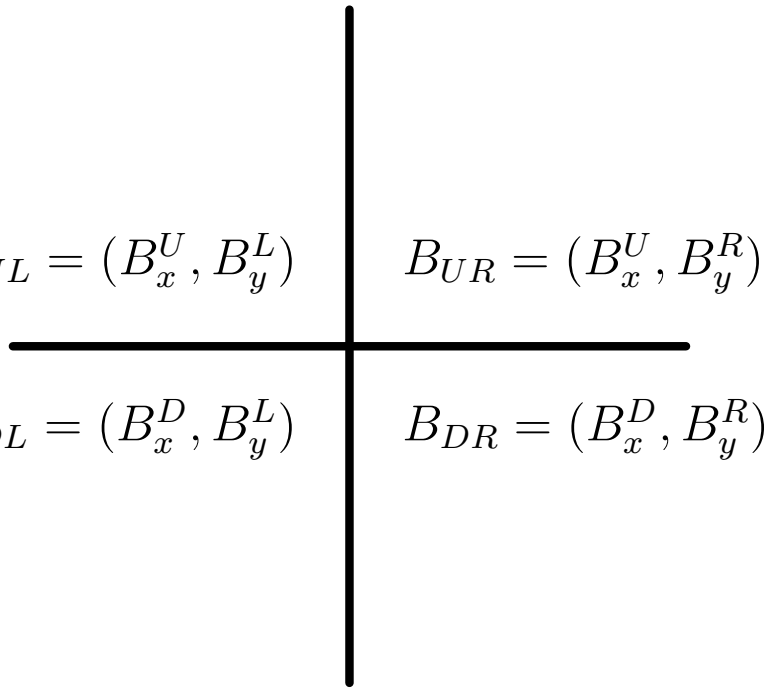

The corner flux is given by

$$\tilde{E} = \begin{cases} E_{DL} & \text{if } v_x > 0,\ v_y > 0 \\ E_{UL} & \text{if } v_x > 0,\ v_y < 0 \\ E_{DR} & \text{if } v_x < 0,\ v_y > 0 \\ E_{UR} & \text{if } v_x < 0,\ v_y < 0 \end{cases}$$

which can be written in compact form as

$$\tilde{E} = \frac{v_y}{2}(B_x^U + B_x^D) - \frac{v_x}{2}(B_y^L + B_y^R) - \frac{|v_y|}{2}\left(B_x^U - B_x^D\right) + \frac{|v_x|}{2}\left(B_y^R - B_y^L\right)$$

Numerical fluxes

An equivalent expression is given by [11]

$$\begin{aligned}\tilde{E} =& \frac{v_y}{4}(B_x^{UL} + B_x^{UR} + B_x^{DL} + B_x^{DR}) - \frac{v_x}{4}(B_y^{UL} + B_y^{UR} + B_y^{DL} + B_y^{DR}) \\ & - \frac{|v_y|}{2}\left(\frac{B_x^{UL} + B_x^{UR}}{2} - \frac{B_x^{DL} + B_x^{DR}}{2}\right) \\ & + \frac{|v_x|}{2}\left(\frac{B_y^{UR} + B_y^{DR}}{2} - \frac{B_y^{UL} + B_y^{DL}}{2}\right)\end{aligned}$$

with the understanding that $B_x^{DL} = B_x^{DR}$, etc.

Boundary flux

$\hat{E}$: Given boundary condition $\boldsymbol{B}^*$

$$\hat{E} = \begin{cases} E(\boldsymbol{B}_{int}, \boldsymbol{v}) & \boldsymbol{v} \cdot \boldsymbol{n} > 0 \\ E(\boldsymbol{B}^*, \boldsymbol{v}) & \text{otherwise} \end{cases}$$

$\tilde{E}$: Corner flux for boundary point: use numerical flux

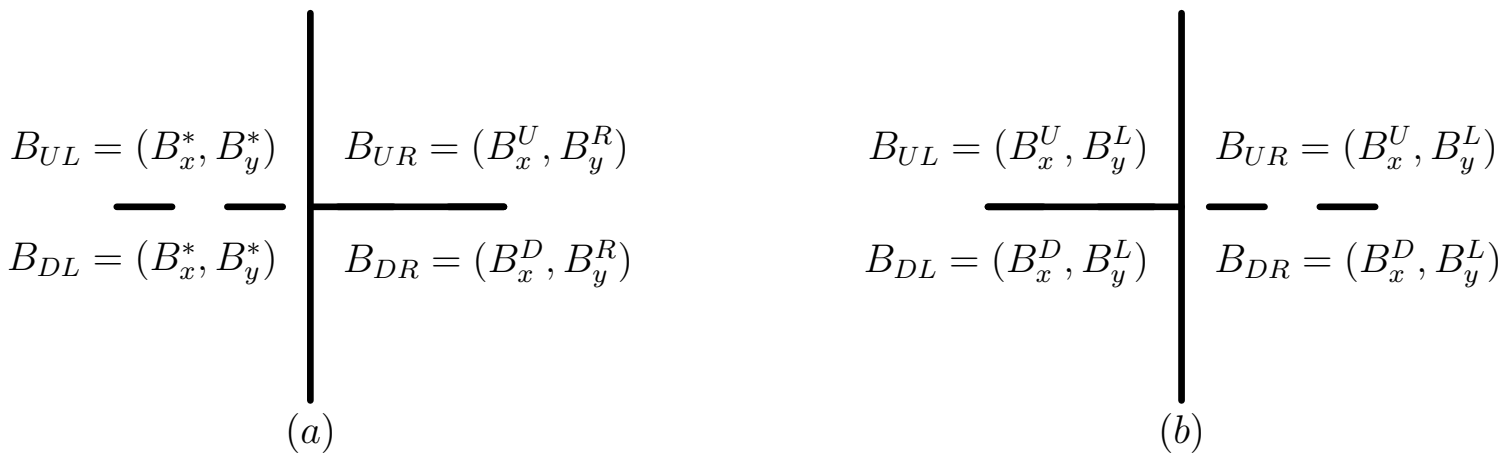

Vertex states at boundary: (a) inflow vertex on left side of domain, (b) outflow vertex on right side of domain

Implementation details

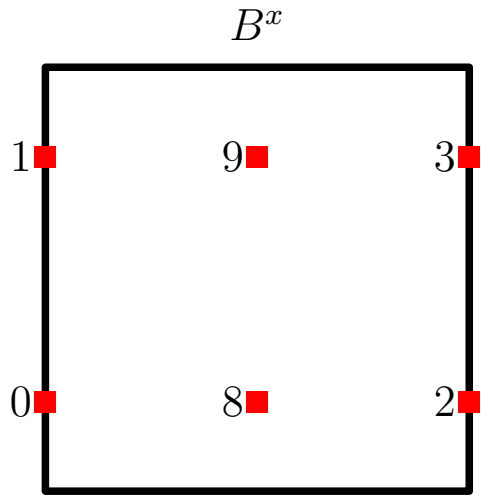

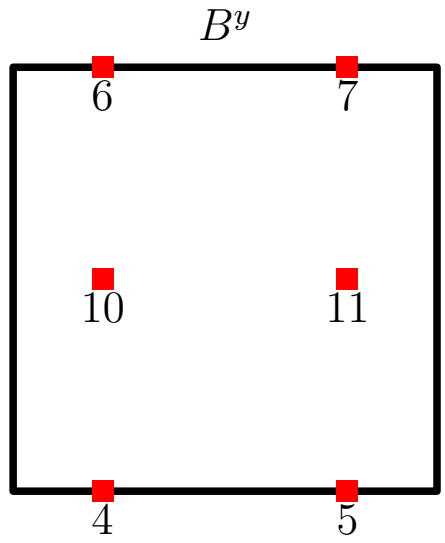

$$\begin{bmatrix} M^x & 0 & 0 & 0 & 0 & 0 \\ 0 & M^x & 0 & 0 & 0 & 0 \\ 0 & 0 & M^y & 0 & 0 & 0 \\ 0 & 0 & 0 & M^y & 0 & 0 \\ N_l^x & N_r^x & 0 & 0 & Q^x & 0 \\ 0 & 0 & N_b^y & N_t^y & 0 & Q^y \end{bmatrix}$$

Numerical Results

- Edge quadrature using $(k+2)$-point GL rule
- Cell quadrature using $(k+2) \times (k+2)$-point GL rule
- Time integration by 3-stage, 3-rd order SSPRK
- Time step

$$\Delta t < \frac{1}{(2k+1)\max\left(\frac{|v_x|}{\Delta x} + \frac{|v_y|}{\Delta y}\right)}$$

- Code written using `deal.II` library

Test 1a: Approximation property

Take $\boldsymbol{B} = (\partial_x \Phi, -\partial_x \Phi)$ where

$$\Phi(x, y) = \sin(2\pi x)\sin(2\pi y), \qquad (x, y) \in [0, 1] \times [0, 1]$$

h	$\|B - B_h\|_{L^2(\Omega)}$		$\|div(B_h)\|_{L^2(\Omega)}$	
0.1250	1.0189e-01	-	3.7147e-14	$k = 1$
0.0625	2.5519e-02	2.00	9.5162e-14	
0.0312	6.3826e-03	2.00	3.7880e-13	
0.0156	1.5958e-03	2.00	1.4840e-12	
0.0078	3.9896e-04	2.00	5.8016e-12	

h	$\|B - B_h\|_{L^2(\Omega)}$		$\|div(B_h)\|_{L^2(\Omega)}$	
0.1250	6.7521e-03	-	1.3265e-13	$k = 2$
0.0625	8.4659e-04	3.00	3.7389e-13	
0.0312	1.0590e-04	3.00	1.3266e-12	
0.0156	1.3241e-05	3.00	5.2716e-12	
0.0078	1.6552e-06	3.00	2.0924e-11	

Test 1b: Approximation property

$\boldsymbol{B} = \nabla\Phi$ where

$$\Phi(x,y) = \frac{1}{10}\exp[-20(x^2+y^2)], \qquad (x,y) \in [-1,+1]\times[-1,+1]$$

h	$\|B - B_h\|_{L^2(\Omega)}$		$\|div(B) - div(B_h)\|_{L^2(\Omega)}$		
0.0625	9.0930e-04	-	2.7438e-02	-	
0.0312	2.2445e-04	2.02	6.9076e-03	1.99	$k=1$
0.0156	5.5927e-05	2.00	1.7299e-03	2.00	
0.0078	1.3970e-05	2.00	4.3267e-04	2.00	
0.0039	3.4918e-06	2.00	1.0818e-04	2.00	

h	$\|B - B_h\|_{L^2(\Omega)}$		$\|div(B) - div(B_h)\|_{L^2(\Omega)}$		
0.0625	4.7750e-05	-	1.8703e-03	-	
0.0312	5.9190e-06	3.01	2.3550e-04	2.99	$k=2$
0.0156	7.3827e-07	3.00	2.9491e-05	3.00	
0.0078	9.2233e-08	3.00	3.6881e-06	3.00	
0.0039	1.1528e-08	3.00	4.6106e-07	3.00	

Test 2: Smooth test case

The initial condition is given by $\boldsymbol{B}_0 = (\partial_y \Phi, -\partial_x \Phi)$ where

$$\Phi(x, y) = \frac{1}{10} \exp[-20((x - 1/2)^2 + y^2)]$$

and the velocity field is $\boldsymbol{v} = (y, -x)$. The exact solution is a pure rotation of the initial condition and is given by

$$\boldsymbol{B}(\boldsymbol{r}, t) = R(t)\boldsymbol{B}_0(R(-t)\boldsymbol{r}), \qquad R(t) = \begin{bmatrix} \cos t & -\sin t \\ \sin t & \cos t \end{bmatrix}$$

Animation

Test 2a: Smooth test case

We compute the numerical solution on the computational domain $[-1, +1] \times [-1, +1]$ upto a final time of $T = 2\pi$ at which time the solution comes back to the initial condition.

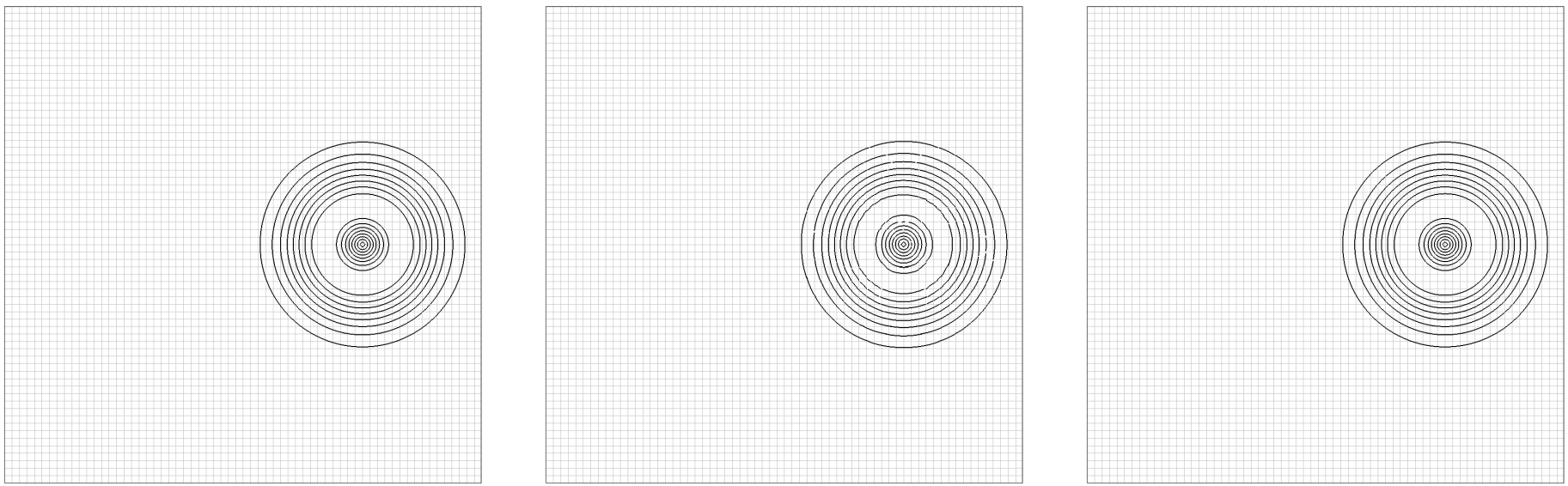

(a) (b) (c)

Contour of $|\boldsymbol{B}_h|$ for Test 2a, 10 contours between 0 and 0.3867: (a) initial, (b) final, $k = 1$, (c) final, $k = 2$

Test 2a: Smooth test case

h	$\|\boldsymbol{B}_h - \boldsymbol{B}\|_{L^2(\Omega)}$		$\|div(\boldsymbol{B}_h)\|_{L^2(\Omega)}$	
0.0312	2.1427e-03	-	6.0137e-14	
0.0156	3.2571e-04	2.71	1.8566e-13	$k = 1$
0.0078	5.9640e-05	2.45	5.8486e-13	
0.0039	1.3209e-05	2.17	1.8853e-12	

h	$\|\boldsymbol{B}_h - \boldsymbol{B}\|_{L^2(\Omega)}$		$\|div(\boldsymbol{B}_h)\|_{L^2(\Omega)}$	
0.0625	2.4003e-04	-	4.9081e-14	
0.0312	2.5212e-05	3.25	1.4299e-13	$k = 2$
0.0156	3.0946e-06	3.02	4.5663e-13	
0.0078	3.8448e-07	3.00	1.5058e-12	

Test 2b: Smooth test case

We compute the numerical solution on the computational domain $[0, 1] \times [0, 1]$ upto a final time of $T = \pi/4$.

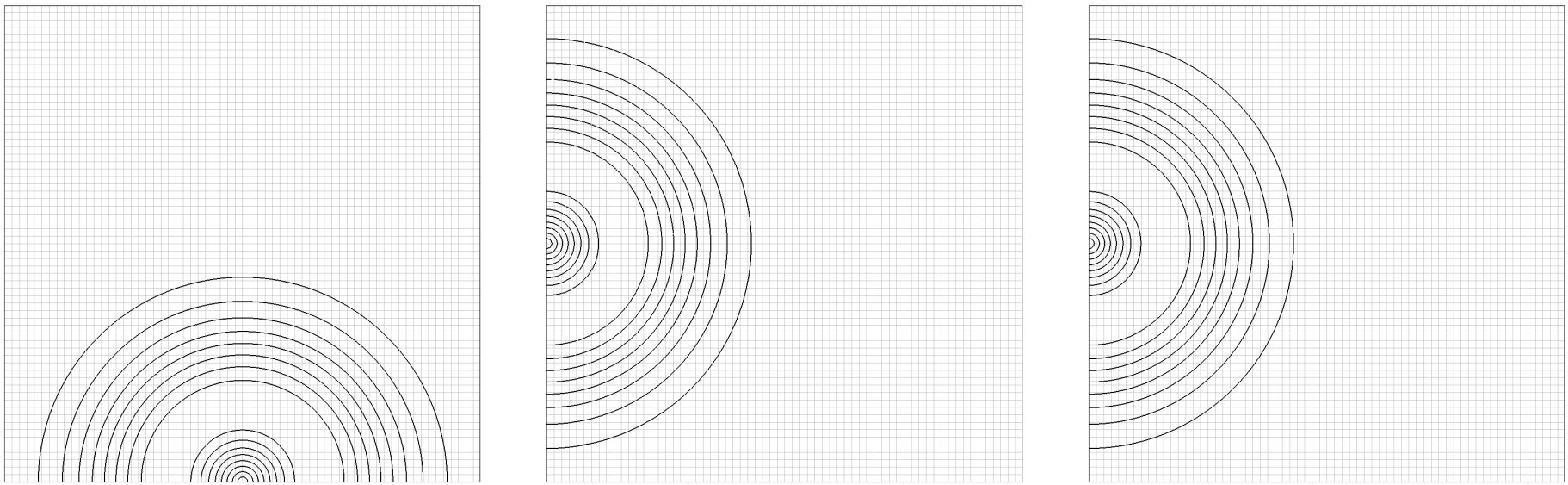

(a) (b) (c)

Contour of $|\boldsymbol{B}_h|$ for Test 2b, 10 contours between 0 and 0.3867: (a) initial, (b) final, $k = 1$, (c) final, $k = 2$

Test 2b: Smooth test case

h	$\|\boldsymbol{B}_h - \boldsymbol{B}\|_{L^2(\Omega)}$		$\|div(\boldsymbol{B}_h)\|_{L^2(\Omega)}$	
0.0312	6.5882e-04	-	2.8687e-14	
0.0156	1.4979e-04	2.13	9.8666e-14	$k = 1$
0.0078	3.6394e-05	2.04	3.2902e-13	
0.0039	9.0308e-06	2.01	1.1356e-12	

h	$\|\boldsymbol{B}_h - \boldsymbol{B}\|_{L^2(\Omega)}$		$\|div(\boldsymbol{B}_h)\|_{L^2(\Omega)}$	
0.0625	1.4110e-04	-	2.4986e-14	
0.0312	1.7238e-05	3.03	7.9129e-14	$k = 2$
0.0156	2.1442e-06	3.00	2.5910e-13	
0.0078	2.6749e-07	3.00	9.2720e-13	

Test 3: Smooth test case, divergent solution

The exact solution is taken to be

$$\boldsymbol{B}(x, y, t) = \begin{bmatrix} \cos t & -\sin t \\ \sin t & \cos t \end{bmatrix} \boldsymbol{B}_0(x, y)$$

where

$$\boldsymbol{B}_0 = \nabla\phi, \qquad \phi = \frac{1}{10}\exp(-20(x^2 + y^2))$$

so that $\nabla \cdot \boldsymbol{B} \neq 0$, and the velocity field is taken as

$$\boldsymbol{v} = \nabla^\top \psi, \qquad \psi = \frac{1}{\pi}\sin(\pi x)\sin(\pi y)$$

The right hand side source term $\boldsymbol{M}$ is computed from the above solution using the formula $\boldsymbol{M} = -\frac{\partial \boldsymbol{B}}{\partial t} + \nabla \times (\boldsymbol{v} \times \boldsymbol{B})$. The problem is solved on the domain $[-1, +1] \times [-1, +1]$ until a final time of $T = 2\pi$.

Test 3: Smooth test case, divergent solution

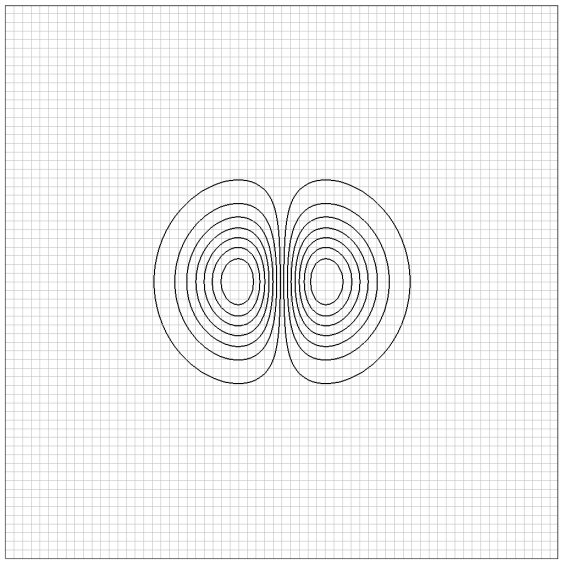

(a)

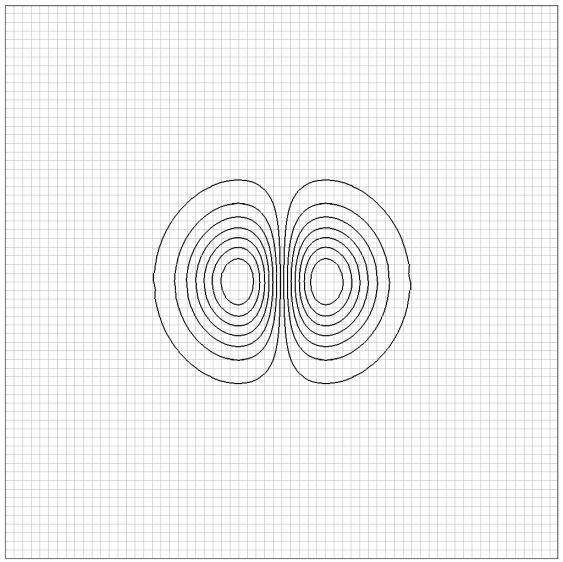

(b)

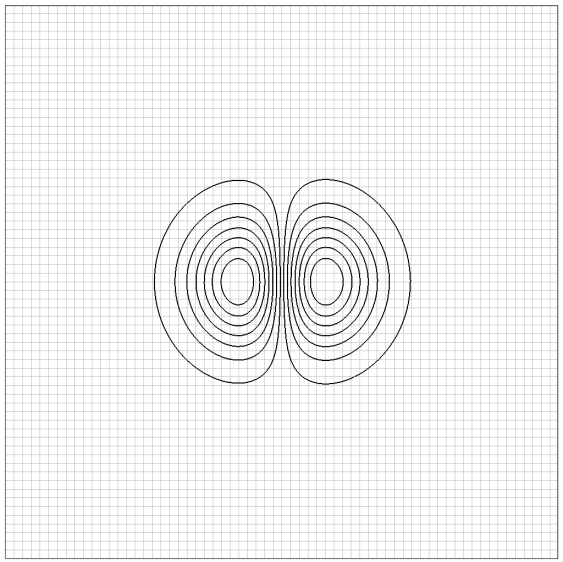

(c)

Contour plot of B_x for Test 3 showing 16 contours between -0.3838 and +0.3838: (a) initial condition, (b) final, $k = 1$ and (c) final, $k = 2$

Test 3: Smooth test case, divergent solution

h	$\|\boldsymbol{B}_h - \boldsymbol{B}\|_{L^2(\Omega)}$		$\|div(\boldsymbol{B}) - div(\boldsymbol{B}_h)\|_{L^2(\Omega)}$		
0.0312	8.5550e-04	-	6.9076e-03	-	
0.0156	1.8915e-04	2.17	1.7299e-03	1.99	$k = 1$
0.0078	3.8730e-05	2.29	4.3267e-04	1.99	
0.0039	7.8346e-06	2.30	1.0818e-04	1.99	

h	$\|\boldsymbol{B}_h - \boldsymbol{B}\|_{L^2(\Omega)}$		$\|div(\boldsymbol{B}) - div(\boldsymbol{B}_h)\|_{L^2(\Omega)}$		
0.0625	3.4775e-04	-	1.8703e-03	-	
0.0312	3.3408e-05	3.38	2.3550e-04	2.99	$k = 2$
0.0156	3.0287e-06	3.46	2.9491e-05	2.99	
0.0078	2.7345e-07	3.47	3.6881e-06	2.99	

Test 4: Discontinuous test case

We take the potential

$$\Phi(x,y) = \begin{cases} 2y - 2x & x > y \\ 0 & \text{otherwise} \end{cases}$$

and the velocity field is $\boldsymbol{v} = (1,2)$. This leads to a discontinuous magnetic field with the discontinuity along the line $x = y$

$$\boldsymbol{B}_0 = \begin{cases} (2,2) & x > y \\ (0,0) & x < y \end{cases}$$

The exact solution is given by

$$\boldsymbol{B}(x,y,t) = \boldsymbol{B}_0(x - t, y - 2t)$$

Animation

Test 4: Discontinuous test case

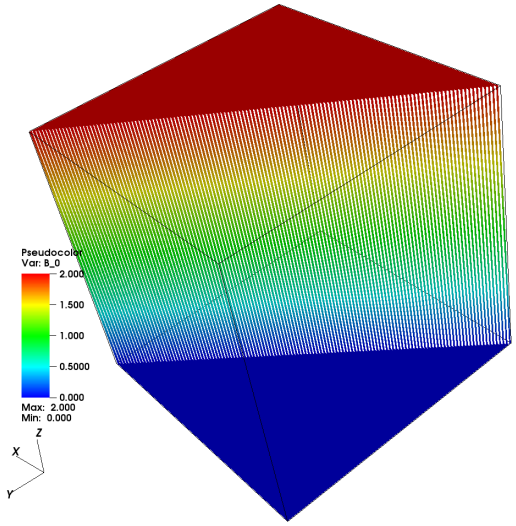

(a) IC

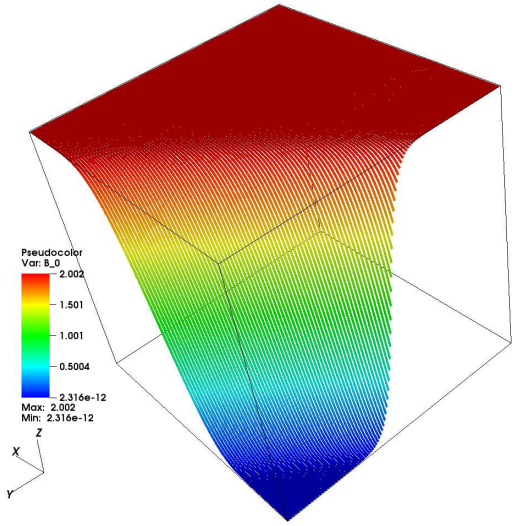

(b) $k = 0$

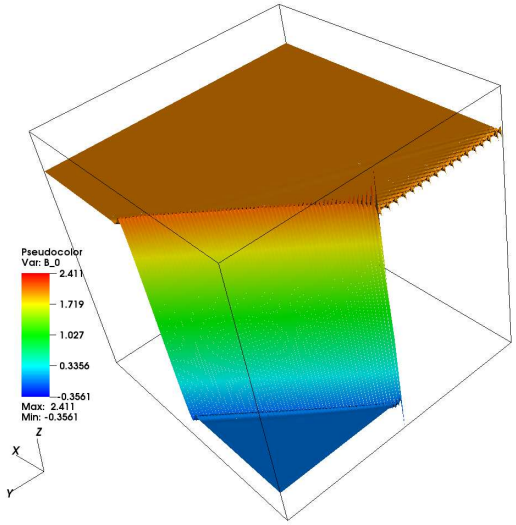

(c) $k = 1$

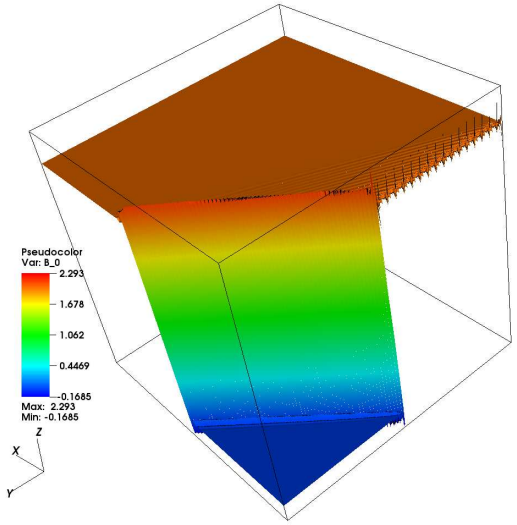

(d) $k = 2$

Summary

- DG scheme on Cartesian meshes
- Globally divergence-free solutions
- Arbitrary orders possible
- Local mass matrices: good for explicit time-stepping

Ongoing work

- Adaptive mesh refinement
- Unstructured grids
- Limiters
- Application to
  - Maxwell equations (CED)
  - Magnetohydrodynamics (MHD)

Ongoing work

- Adaptive mesh refinement
- Unstructured grids
- Limiters
- Application to
  - Maxwell equations (CED)
  - Magnetohydrodynamics (MHD)

Thank You

References

[1] C. R. Evans, J. F. Hawley, Simulation of magnetohydrodynamic flows - A constrained transport method, Astrophysical Journal 332 (1988) 659–677.
doi:10.1086/166684.

[2] D. S. Balsara, Divergence-free adaptive mesh refinement for magnetohydrodynamics, Journal of Computational Physics 174 (2) (2001) 614 – 648.
doi:http://dx.doi.org/10.1006/jcph.2001.6917.
URL http://www.sciencedirect.com/science/article/pii/S0021999101969177

References

[3] F. Li, L. Xu, S. Yakovlev, Central discontinuous galerkin methods for ideal MHD equations with the exactly divergence-free magnetic field, Journal of Computational Physics 230 (12) (2011) 4828 – 4847. doi:http://dx.doi.org/10.1016/j.jcp.2011.03.006.
URL http://www.sciencedirect.com/science/article/pii/S0021999111001495

[4] S. K. Godunov, The symmetric form of magnetohydrodynamics equation, Num. Meth. Mech. Cont. Media 34 (1972) 1–26.

[5] K. Powell, An approximate Riemann solver for magnetohydrodynamics (that works in more than one dimension), Tech. Rep. 94-24, ICASE, NASA Langley (1994).

References

[6] P. Chandrashekar, C. Klingenberg, Entropy stable finite volume scheme for ideal compressible mhd on 2-d cartesian meshes, SIAM Journal on Numerical Analysis 54 (2) (2016) 1313–1340.
arXiv:https://doi.org/10.1137/15M1013626,
doi:10.1137/15M1013626.
URL https://doi.org/10.1137/15M1013626

[7] A. Dedner, F. Kemm, D. Kröner, C.-D. Munz, T. Schnitzer, M. Wesenberg, Hyperbolic divergence cleaning for the MHD equations, Journal of Computational Physics 175 (2) (2002) 645 – 673.
doi:http://dx.doi.org/10.1006/jcph.2001.6961.
URL http://www.sciencedirect.com/science/article/pii/S002199910196961X

[8] A. M. Quarteroni, A. Valli, Numerical Approximation of Partial Differential Equations, 1st Edition, Springer Publishing Company, Incorporated, 2008.

References

[9] F. Brezzi, M. Fortin, Mixed and Hybrid Finite Element Methods, Springer-Verlag New York, Inc., New York, NY, USA, 1991.

[10] D. N. Arnold, D. Boffi, R. S. Falk, Quadrilateral H(div) finite elements, SIAM Journal on Numerical Analysis 42 (6) (2005) 2429–2451.
arXiv:https://doi.org/10.1137/S0036142903431924,
doi:10.1137/S0036142903431924.
URL https://doi.org/10.1137/S0036142903431924

[11] D. S. Balsara, R. Käppeli, Von Neumann stability analysis of globally divergence-free RKDG schemes for the induction equation using multidimensional riemann solvers, Journal of Computational Physics 336 (2017) 104 – 127.

References

doi:https://doi.org/10.1016/j.jcp.2017.01.056.
URL http://www.sciencedirect.com/science/article/pii/S0021999117300724